



# Measurement of the Electroweak Penguin Process

## $B \rightarrow X_s \ell^+ \ell^-$

J. Kaneko,<sup>47</sup> K. Abe,<sup>9</sup> K. Abe,<sup>44</sup> T. Abe,<sup>45</sup> I. Adachi,<sup>9</sup> Byoung Sup Ahn,<sup>16</sup> H. Aihara,<sup>46</sup> M. Akatsu,<sup>23</sup> Y. Asano,<sup>51</sup> T. Aso,<sup>50</sup> V. Aulchenko,<sup>2</sup> T. Aushev,<sup>13</sup> A. M. Bakich,<sup>41</sup> Y. Ban,<sup>34</sup> E. Banas,<sup>28</sup> W. Bartel,<sup>6</sup> A. Bay,<sup>19</sup> P. K. Behera,<sup>52</sup> A. Bondar,<sup>2</sup> A. Bozek,<sup>28</sup> M. Bračko,<sup>21,14</sup> J. Brodzicka,<sup>28</sup> T. E. Browder,<sup>8</sup> B. C. K. Casey,<sup>8</sup> P. Chang,<sup>27</sup> Y. Chao,<sup>27</sup> K.-F. Chen,<sup>27</sup> B. G. Cheon,<sup>40</sup> R. Chistov,<sup>13</sup> Y. Choi,<sup>40</sup> Y. K. Choi,<sup>40</sup> M. Danilov,<sup>13</sup> L. Y. Dong,<sup>11</sup> S. Eidelman,<sup>2</sup> V. Eiges,<sup>13</sup> Y. Enari,<sup>23</sup> C. W. Everton,<sup>22</sup> F. Fang,<sup>8</sup> H. Fujii,<sup>9</sup> C. Fukunaga,<sup>48</sup> N. Gabyshev,<sup>9</sup> A. Garmash,<sup>2,9</sup> T. Gershon,<sup>9</sup> R. Guo,<sup>25</sup> J. Haba,<sup>9</sup> F. Handa,<sup>45</sup> T. Hara,<sup>32</sup> Y. Harada,<sup>30</sup> N. C. Hastings,<sup>22</sup> H. Hayashii,<sup>24</sup> M. Hazumi,<sup>9</sup> E. M. Heenan,<sup>22</sup> I. Higuchi,<sup>45</sup> T. Higuchi,<sup>46</sup> L. Hinz,<sup>19</sup> T. Hojo,<sup>32</sup> Y. Hoshi,<sup>44</sup> W.-S. Hou,<sup>27</sup> H.-C. Huang,<sup>27</sup> T. Igaki,<sup>23</sup> Y. Igarashi,<sup>9</sup> T. Iijima,<sup>23</sup> K. Inami,<sup>23</sup> A. Ishikawa,<sup>23</sup> H. Ishino,<sup>47</sup> R. Itoh,<sup>9</sup> H. Iwasaki,<sup>9</sup> Y. Iwasaki,<sup>9</sup> H. K. Jang,<sup>39</sup> J. H. Kang,<sup>55</sup> J. S. Kang,<sup>16</sup> N. Katayama,<sup>9</sup> H. Kawai,<sup>3</sup> Y. Kawakami,<sup>23</sup> N. Kawamura,<sup>1</sup> T. Kawasaki,<sup>30</sup> H. Kichimi,<sup>9</sup> D. W. Kim,<sup>40</sup> Heejong Kim,<sup>55</sup> H. J. Kim,<sup>55</sup> H. O. Kim,<sup>40</sup> Hyunwoo Kim,<sup>16</sup> S. K. Kim,<sup>39</sup> K. Kinoshita,<sup>5</sup> S. Kobayashi,<sup>37</sup> S. Korpar,<sup>21,14</sup> P. Križan,<sup>20,14</sup> P. Krokovny,<sup>2</sup> R. Kulasiri,<sup>5</sup> S. Kumar,<sup>33</sup> Y.-J. Kwon,<sup>55</sup> J. S. Lange,<sup>7,36</sup> G. Leder,<sup>12</sup> S. H. Lee,<sup>39</sup> J. Li,<sup>38</sup> A. Limosani,<sup>22</sup> R.-S. Lu,<sup>27</sup> J. MacNaughton,<sup>12</sup> G. Majumder,<sup>42</sup> F. Mandl,<sup>12</sup> D. Marlow,<sup>35</sup> S. Matsumoto,<sup>4</sup> T. Matsumoto,<sup>48</sup> W. Mitaroff,<sup>12</sup> K. Miyabayashi,<sup>24</sup> Y. Miyabayashi,<sup>23</sup> H. Miyake,<sup>32</sup> G. R. Moloney,<sup>22</sup> T. Mori,<sup>4</sup> T. Nagamine,<sup>45</sup> Y. Nagasaka,<sup>10</sup> T. Nakadaira,<sup>46</sup> E. Nakano,<sup>31</sup> M. Nakao,<sup>9</sup> J. W. Nam,<sup>40</sup> K. Neichi,<sup>44</sup> S. Nishida,<sup>17</sup> O. Nitoh,<sup>49</sup> S. Noguchi,<sup>24</sup> T. Nozaki,<sup>9</sup> S. Ogawa,<sup>43</sup> T. Ohshima,<sup>23</sup> T. Okabe,<sup>23</sup> S. Okuno,<sup>15</sup> S. L. Olsen,<sup>8</sup> Y. Onuki,<sup>30</sup> W. Ostrowicz,<sup>28</sup> H. Ozaki,<sup>9</sup> P. Pakhlov,<sup>13</sup> H. Palka,<sup>28</sup> C. W. Park,<sup>16</sup> H. Park,<sup>18</sup> K. S. Park,<sup>40</sup> J.-P. Perroud,<sup>19</sup> M. Peters,<sup>8</sup> L. E. Piilonen,<sup>53</sup> N. Root,<sup>2</sup> K. Rybicki,<sup>28</sup> H. Sagawa,<sup>9</sup> Y. Sakai,<sup>9</sup> H. Sakamoto,<sup>17</sup> M. Satapathy,<sup>52</sup> A. Satpathy,<sup>9,5</sup> O. Schneider,<sup>19</sup> S. Schrenk,<sup>5</sup> C. Schwanda,<sup>9,12</sup> S. Semenov,<sup>13</sup> K. Senyo,<sup>23</sup> R. Seuster,<sup>8</sup> H. Shibuya,<sup>43</sup> B. Shwartz,<sup>2</sup> V. Sidorov,<sup>2</sup> J. B. Singh,<sup>33</sup> N. Soni,<sup>33</sup> S. Stanič,<sup>51,\*</sup> K. Sumisawa,<sup>9</sup> T. Sumiyoshi,<sup>48</sup> K. Suzuki,<sup>9</sup> S. Suzuki,<sup>54</sup> S. Y. Suzuki,<sup>9</sup> S. K. Swain,<sup>8</sup> H. Tajima,<sup>46</sup> T. Takahashi,<sup>31</sup> F. Takasaki,<sup>9</sup> K. Tamai,<sup>9</sup> N. Tamura,<sup>30</sup> J. Tanaka,<sup>46</sup> M. Tanaka,<sup>9</sup> G. N. Taylor,<sup>22</sup> Y. Teramoto,<sup>31</sup> S. Tokuda,<sup>23</sup> M. Tomoto,<sup>9</sup> T. Tomura,<sup>46</sup> K. Trabelsi,<sup>8</sup> W. Trischuk,<sup>35,†</sup> T. Tsuboyama,<sup>9</sup> T. Tsukamoto,<sup>9</sup> S. Uehara,<sup>9</sup> K. Ueno,<sup>27</sup> S. Uno,<sup>9</sup> Y. Ushiroda,<sup>9</sup> G. Varner,<sup>8</sup> K. E. Varvell,<sup>41</sup> C. C. Wang,<sup>27</sup> C. H. Wang,<sup>26</sup> J. G. Wang,<sup>53</sup> M.-Z. Wang,<sup>27</sup> Y. Watanabe,<sup>47</sup> E. Won,<sup>16</sup> B. D. Yabsley,<sup>53</sup> Y. Yamada,<sup>9</sup> A. Yamaguchi,<sup>45</sup> Y. Yamashita,<sup>29</sup> M. Yamauchi,<sup>9</sup> H. Yanai,<sup>30</sup> J. Yashima,<sup>9</sup> M. Yokoyama,<sup>46</sup> Y. Yuan,<sup>11</sup> Y. Yusa,<sup>45</sup> C. C. Zhang,<sup>11</sup> J. Zhang,<sup>51</sup> Z. P. Zhang,<sup>38</sup> Y. Zheng,<sup>8</sup> V. Zhilich,<sup>2</sup> and D. Žontar<sup>51</sup>

(The Belle Collaboration)

<sup>1</sup>Aomori University, Aomori

<sup>2</sup>*Budker Institute of Nuclear Physics, Novosibirsk*  
<sup>3</sup>*Chiba University, Chiba*  
<sup>4</sup>*Chuo University, Tokyo*  
<sup>5</sup>*University of Cincinnati, Cincinnati OH*  
<sup>6</sup>*Deutsches Elektronen-Synchrotron, Hamburg*  
<sup>7</sup>*University of Frankfurt, Frankfurt*  
<sup>8</sup>*University of Hawaii, Honolulu HI*  
<sup>9</sup>*High Energy Accelerator Research Organization (KEK), Tsukuba*  
<sup>10</sup>*Hiroshima Institute of Technology, Hiroshima*  
<sup>11</sup>*Institute of High Energy Physics,  
Chinese Academy of Sciences, Beijing*  
<sup>12</sup>*Institute of High Energy Physics, Vienna*  
<sup>13</sup>*Institute for Theoretical and Experimental Physics, Moscow*  
<sup>14</sup>*J. Stefan Institute, Ljubljana*  
<sup>15</sup>*Kanagawa University, Yokohama*  
<sup>16</sup>*Korea University, Seoul*  
<sup>17</sup>*Kyoto University, Kyoto*  
<sup>18</sup>*Kyungpook National University, Taegu*  
<sup>19</sup>*Institut de Physique des Hautes Énergies, Université de Lausanne, Lausanne*  
<sup>20</sup>*University of Ljubljana, Ljubljana*  
<sup>21</sup>*University of Maribor, Maribor*  
<sup>22</sup>*University of Melbourne, Victoria*  
<sup>23</sup>*Nagoya University, Nagoya*  
<sup>24</sup>*Nara Women's University, Nara*  
<sup>25</sup>*National Kaohsiung Normal University, Kaohsiung*  
<sup>26</sup>*National Lien-Ho Institute of Technology, Miao Li*  
<sup>27</sup>*National Taiwan University, Taipei*  
<sup>28</sup>*H. Niewodniczanski Institute of Nuclear Physics, Krakow*  
<sup>29</sup>*Nihon Dental College, Niigata*  
<sup>30</sup>*Niigata University, Niigata*  
<sup>31</sup>*Osaka City University, Osaka*  
<sup>32</sup>*Osaka University, Osaka*  
<sup>33</sup>*Panjab University, Chandigarh*  
<sup>34</sup>*Peking University, Beijing*  
<sup>35</sup>*Princeton University, Princeton NJ*  
<sup>36</sup>*RIKEN BNL Research Center, Brookhaven NY*  
<sup>37</sup>*Saga University, Saga*  
<sup>38</sup>*University of Science and Technology of China, Hefei*  
<sup>39</sup>*Seoul National University, Seoul*  
<sup>40</sup>*Sungkyunkwan University, Suwon*  
<sup>41</sup>*University of Sydney, Sydney NSW*  
<sup>42</sup>*Tata Institute of Fundamental Research, Bombay*  
<sup>43</sup>*Toho University, Funabashi*  
<sup>44</sup>*Tohoku Gakuin University, Tagajo*  
<sup>45</sup>*Tohoku University, Sendai*  
<sup>46</sup>*University of Tokyo, Tokyo*  
<sup>47</sup>*Tokyo Institute of Technology, Tokyo*

<sup>48</sup>*Tokyo Metropolitan University, Tokyo*

<sup>49</sup>*Tokyo University of Agriculture and Technology, Tokyo*

<sup>50</sup>*Toyama National College of Maritime Technology, Toyama*

<sup>51</sup>*University of Tsukuba, Tsukuba*

<sup>52</sup>*Utkal University, Bhubaneswar*

<sup>53</sup>*Virginia Polytechnic Institute and State University, Blacksburg VA*

<sup>54</sup>*Yokkaichi University, Yokkaichi*

<sup>55</sup>*Yonsei University, Seoul*

(Dated: August 19, 2002)

## Abstract

We report the first measurement of the branching fraction for the inclusive decay  $B \rightarrow X_s \ell^+ \ell^-$ , where  $\ell$  is either an electron or a muon and  $X_s$  is a hadronic recoil system that contains a kaon. We analyzed a data sample of  $65.4 \times 10^6$   $B$  meson pairs collected with the Belle detector at the KEKB  $e^+e^-$  asymmetric-energy collider. We find  $\mathcal{B}(B \rightarrow X_s \ell^+ \ell^-) = (6.1 \pm 1.4(\text{stat})^{+1.4}_{-1.1}(\text{syst})) \times 10^{-6}$  for dilepton masses greater than 0.2 GeV/ $c^2$ .

PACS numbers: 13.20.He, 14.65.Fy, 14.40.Nd

The first observation of the flavor-changing neutral current process  $b \rightarrow s\ell^+\ell^-$  in the decay  $B \rightarrow K\ell^+\ell^-$  by Belle [1] recently opened a new window on the search for physics beyond the Standard Model (SM) [2]. In the SM, the lowest order diagrams for  $b \rightarrow s\ell^+\ell^-$  are loop (electroweak and electromagnetic penguins) and box diagrams of a virtual top quark and a weak boson. In general, non-SM tree diagrams or non-SM particles (such as charged Higgs or SUSY particles) participating in the loop and box diagrams can produce a sizeable modification to the SM decay amplitude, for which the next-to-next-to-leading order (NNLO) corrections have been calculated [3]. The decay amplitude is often described with an effective Hamiltonian, in which the non-SM contributions are considered as modifications to the Wilson coefficients,  $C_7$ ,  $C_9$  and  $C_{10}$ . The size of the coefficient  $C_7$  has been constrained from the measured  $B \rightarrow X_s\gamma$  rate [4, 5, 6]. Our previous  $B \rightarrow K\ell^+\ell^-$  measurement has already provided the best limit on the non-SM contributions to  $C_9$  and  $C_{10}$  [7]; however, measurements of the inclusive branching fraction and the dilepton and recoil mass spectra will provide a more stringent and model independent probe for new physics.

In this Letter, we present the results of a measurement of the branching fraction for the inclusive decay  $B \rightarrow X_s\ell^+\ell^-$ , where  $B$  is either  $B^0$  or  $B^+$ ,  $\ell$  is either an electron or a muon, and  $X_s$  is a hadronic recoil system that contains a kaon. Here and throughout the paper, the inclusion of charge conjugated modes is implied. We use a data sample collected at the  $\Upsilon(4S)$  resonance with the Belle detector at the KEKB  $e^+e^-$  asymmetric-energy collider (3.5 GeV on 8 GeV) [8]. The data sample contains  $(65.4 \pm 0.5) \times 10^6$   $B$  meson pairs, corresponding to an integrated luminosity of  $60 \text{ fb}^{-1}$ .

The Belle detector is a large-solid-angle magnetic spectrometer that consists of a three-layer silicon vertex detector (SVD), a 50-layer central drift chamber (CDC), an array of aerogel threshold Čerenkov counters (ACC), time-of-flight scintillation counters (TOF), and an electromagnetic calorimeter comprised of CsI(Tl) crystals (ECL) located inside a superconducting solenoid coil that provides a 1.5 T magnetic field. An iron flux-return located outside of the coil is instrumented with resistive plate counters to identify muons (KLM). The detector is described in detail elsewhere [9].

We reconstruct charged particle trajectories with the CDC and SVD. Electron identification is based on the position and shower shape of the cluster in the ECL, ratio of the cluster energy to the track momentum ( $E/p$ ), specific energy-loss measurement ( $dE/dx$ ) with the CDC and the response from the ACC. We require the electron's laboratory momentum to be greater than  $0.5 \text{ GeV}/c$ ;  $dE/dx$  separates electrons from other particles between  $0.5 \text{ GeV}/c$  and  $1 \text{ GeV}/c$ , and  $E/p$  provides excellent electron identification above  $1 \text{ GeV}/c$ . We find an electron selection efficiency of 92.5% with a 0.2% pion to electron mis-identification probability. Muon identification is based on the hit positions and depth of the penetration into the ECL and KLM. We require the muon's laboratory momentum to be greater than  $1 \text{ GeV}/c$  to ensure penetration into the KLM. The muon selection efficiency is measured to be 91.3% with a 1.4% pion to muon mis-identification probability. Charged kaon candidates are selected by using a kaon to pion likelihood ratio based on the ACC response,  $dE/dx$  in the CDC and the flight-time measurement with the TOF. The kaon selection efficiency is 90% with a pion to kaon mis-identification probability of 6%. The remaining charged tracks are assumed to be pions. We select  $K_S^0$  candidates from pairs of oppositely charged pions with invariant mass within  $15 \text{ MeV}/c^2$  of the  $K^0$  mass. We impose additional  $K_S^0$  selection criteria based on the distance and the direction of the  $K_S^0$  vertex and the impact parameters of daughter tracks. We require the charged tracks other than those used in the  $K_S^0$  reconstruction to have impact parameters with respect to the nominal interaction point

of less than 0.5 cm in the radial direction and 3 cm along the beam direction.

We reconstruct photons from ECL energy clusters that have no associated charged tracks. The shower shape is required to be consistent with an electromagnetic cluster and the energy to be greater than 50 MeV. We reconstruct  $\pi^0 \rightarrow \gamma\gamma$  candidates from photon pairs with invariant mass within  $10 \text{ MeV}/c^2$  of the nominal  $\pi^0$  mass.

The  $X_s$  system is reconstructed from either a  $K^+$  or  $K^0$  combined with 0 to 4 pions, of which up to one  $\pi^0$  is allowed. This set of combinations covers  $(81 \pm 2)\%$  of the total inclusive decays based on a model discussed below. We reconstruct  $K^0$  candidates only in the  $K^0 \rightarrow K_S^0 \rightarrow \pi^+\pi^-$  channel. We combine the  $X_s$  with two oppositely charged leptons to form a  $B$  candidate. We identify the  $B \rightarrow X_s \ell^+ \ell^-$  signal with the beam-energy constrained mass,  $M_{bc} = \sqrt{(E_{\text{beam}}^{\text{CM}}/c^2)^2 - (p_B^{\text{CM}}/c)^2}$ , where  $E_{\text{beam}}^{\text{CM}}$  and  $p_B^{\text{CM}}$  are the beam energy and magnitude of the  $B$  candidate momentum calculated in the center-of-mass (CM) system, respectively. We find the average  $M_{bc}$  resolution is  $\sigma_{bc} = 2.8 \text{ MeV}/c^2$ . The other independent kinematic variable, the energy difference  $\Delta E = E_B^{\text{CM}} - E_{\text{beam}}^{\text{CM}}$ , where  $E_B^{\text{CM}}$  is the CM energy of the  $B$  candidate, is combined with other variables to provide background suppression.

There are two background sources that are not suppressed by  $M_{bc}$  and  $\Delta E$ . The first is hadronic  $B$  decays into one kaon plus multiple pions ( $B \rightarrow X_s \pi^+ \pi^-$ ) from abundant decays such as  $B \rightarrow D^{(*)} n \pi$  ( $n \geq 1$ ). If we misidentify two of the pions as leptons, we cannot distinguish this background from the signal. We estimate this background contribution by reconstructing  $B \rightarrow X_s \pi^+ \pi^-$  events without the lepton-id criteria and multiplying by the measured momentum dependent mis-identification probability of the pions. We find contributions of  $2.6 \pm 0.2$  events to the  $B \rightarrow X_s \mu^+ \mu^-$  signal and  $0.1 \pm 0.05$  events to  $B \rightarrow X_s e^+ e^-$ . We refer to this as the fake background, and subtract it from the signal yield. The second is from  $B \rightarrow J/\psi X_s$  and  $B \rightarrow \psi' X_s$  where  $J/\psi$  and  $\psi'$  decay into dileptons. These decay modes have the same final states and, in principle, interfere with the signal. For this study, these charmonium decays are explicitly vetoed. The veto windows are  $-0.6$  to  $+0.2 \text{ GeV}/c^2$  ( $-0.35$  to  $+0.2 \text{ GeV}/c^2$ ) around the  $J/\psi$  mass for the  $e^+ e^-$  ( $\mu^+ \mu^-$ ) channel, and  $-0.3$  to  $+0.15 \text{ GeV}/c^2$  around the  $\psi'$  mass for both channels. We apply a wider veto window on the low mass side to suppress  $J/\psi$  and  $\psi'$  candidates in which a photon is radiated from the leptons. After these veto conditions are applied, we estimate from Monte Carlo (MC) that  $0.6$  ( $0.4$ ) background events remain in the signal region of  $M_{bc}$  for  $X_s e^+ e^-$  ( $X_s \mu^+ \mu^-$ ), and find that these events do not produce a signal-like peak.

The largest background sources are random combinations of dileptons with a kaon and pions, from continuum  $q\bar{q}$  ( $q = u, d, s, c$ ) production or from semileptonic  $B$  decays. These two backgrounds do not produce signal-like peaks in  $M_{bc}$  and  $\Delta E$ . The  $q\bar{q}$  background is suppressed by using a Fisher discriminant [10] ( $\mathcal{F}_{\text{cont}}$ ) based on a modified set of Fox-Wolfram moments [11] that differentiate the event topology;  $q\bar{q}$  events are more collimated than  $B$  decay events due to the larger initial quark momenta. We also reject events with a dilepton mass ( $M_{\ell^+ \ell^-}$ ) less than  $0.2 \text{ GeV}/c^2$ , in order to suppress electron pairs from  $\pi^0 \rightarrow e^+ e^- \gamma$  and  $\gamma \rightarrow e^+ e^-$  conversion. In the semileptonic  $B$  decay background, both  $B$  mesons decay into leptons or two leptons are produced from the  $b \rightarrow c \rightarrow s, d$  decay chain. We combine the total visible energy ( $E_{\text{vis}}$ ) of the event and the missing mass ( $M_{\text{miss}}$ ) into another Fisher discriminant ( $\mathcal{F}_{\text{sl}}$ ) to suppress events with two neutrinos.

In addition, we further reduce these backgrounds using  $\Delta E$  and the cosine of the  $B$  flight direction ( $\cos \theta_B$ ) with respect to the  $e^-$  beam direction in the CM frame. First, we select events with  $|\Delta E| < 40 \text{ MeV}$  ( $\sim 3\sigma_{\Delta E}$ ). We then calculate likelihoods  $\mathcal{L}_{S,B} = p_{S,B}^{\Delta E} \times p_{S,B}^{\cos B}$ , where  $p_{S,B}^{\Delta E}$  and  $p_{S,B}^{\cos B}$  are the probability density functions (PDF) for  $\Delta E$  and

$\cos \theta_B$  for the signal ( $S$ ) and the background ( $B$ ), respectively, and form a likelihood ratio  $\mathcal{LR} = \mathcal{L}_S/(\mathcal{L}_S + \mathcal{L}_B)$ . The PDF for the  $\Delta E$  signal is modeled with a Gaussian, and its shape is obtained from a comparison of signal MC,  $B \rightarrow J/\psi X_s$  data and MC; that for the background is modeled with a linear function, and its slope is obtained from a MC sample that contains  $b \rightarrow c$  decays and  $q\bar{q}$  events. The signal follows a  $1 - \cos^2 \theta_B$  distribution, while  $\cos \theta_B$  is almost uniformly populated for the background.

We determine the selection criteria to maximize  $N_S/\sqrt{N_S + N_B}$  for each of  $\mathcal{F}_{\text{cont}}$ ,  $\mathcal{F}_{\text{sl}}$  and  $\mathcal{LR}$  individually in this order, and iterate the procedure to obtain an optimized set of criteria. Here,  $N_S$  is the expected signal yield assuming the predicted SM branching fraction, and  $N_B$  is the expected background yield. We find about 70% of the combinatorial background events that pass these criteria are from semileptonic  $B$  decays.

For events with multiple candidates that pass the selection criteria, we choose the combination with the largest value of  $\mathcal{LR}$ . We then reject candidates with  $X_s$  invariant mass greater than  $2.1 \text{ GeV}/c^2$ . This condition removes a large fraction of combinatorial background while retaining  $(93 \pm 5)\%$  of the signal.

We model the signal characteristics as follows. We use the NNLO calculations of Ref. [7] for the  $M_{\ell^+\ell^-}$  spectrum. We model the recoil mass ( $M_{X_s}$ ) spectrum as a sum of the exclusive  $B \rightarrow K^{(*)}\ell^+\ell^-$  components and an inclusive component based on a Fermi motion model [12] above  $1.1 \text{ GeV}/c^2$ . The quark systems ( $s\bar{d}$  and  $s\bar{u}$ ) are hadronized with the JETSET program [13]. The fractions of  $\pi^0$  and  $K_S^0$  and the events other than the reconstructed combinations are examined to evaluate the hadronization uncertainty. The predicted branching ratios are assumed for the fractions of the exclusive components. The lower boundary of the inclusive component is determined so that the integrated inclusive branching fraction below the boundary of the expected distribution matches the sum of  $B \rightarrow K^{(*)}\ell^+\ell^-$  branching fractions. The largest uncertainty in the  $M_{X_s}$  spectrum is due to the Fermi momentum ( $p_F$ ) and spectator quark mass ( $m_q$ ) parameters. We take  $p_F = 0.4 \text{ GeV}/c$  and  $m_q = 0 \text{ GeV}/c^2$ , and vary the parameters over a range allowed by the measured heavy quark effective theory (HQET) parameters  $\lambda_1$  and  $\overline{\Lambda}$  [5, 14]. The requirement  $M_{\ell^+\ell^-} > 0.2 \text{ GeV}/c^2$  removes the virtual photon contribution,  $b \rightarrow s\gamma^* \rightarrow se^+e^-$ , and makes the predicted rates for the two modes approximately equal:  $\mathcal{B}(B \rightarrow X_s e^+e^-) \sim \mathcal{B}(B \rightarrow X_s \mu^+\mu^-) \sim (4.2 \pm 0.7) \times 10^{-6}$  [15]. Thus we assume an equal branching fraction for the two and take the average to obtain the  $B \rightarrow X_s \ell^+\ell^-$  branching fraction. The expected  $M_{\ell^+\ell^-}$  and  $M_{X_s}$  spectra are shown in Figs. 1(a) and (b), respectively.

Signal MC samples, generated based on this model, are used to determine reconstruction efficiencies of  $(3.9 \pm 0.4 \pm 0.5)\%$  for  $B \rightarrow X_s e^+e^-$  and  $(3.6 \pm 0.4 \pm 0.5)\%$  for  $B \rightarrow X_s \mu^+\mu^-$ , where the first error is systematic and the second error is due to the model uncertainties in the fractions of the exclusive components ( $\sim 11\%$ ), the extrapolation to  $M_{X_s} > 2.1 \text{ GeV}/c^2$  ( $\sim 4\%$ ), and the hadronization (5.1%). Here, an equal production rate is assumed for  $B^0\overline{B}^0$  and  $B^+B^-$ . Systematic errors include uncertainties from the tracking efficiency (2.0% per track),  $K_S^0$  reconstruction efficiency (8.7% per  $K_S^0$ ),  $\pi^0$  reconstruction efficiency (6.8% per  $\pi^0$ ), electron identification (1.8% per electron), muon identification (2.2% per muon),  $K^+$  identification (2.5% per  $K^+$ ),  $\pi^+$  identification (0.8% per  $\pi^+$ ), and the background suppression criteria (3.0% for  $\mathcal{F}_{\text{cont}}$ ,  $\mathcal{F}_{\text{sl}}$  and  $\mathcal{LR}$ , combined).

We determine the signal yield from an unbinned maximum likelihood fit to the  $M_{bc}$  distribution as shown in Fig. 2. We model the signal with a Gaussian function and the background with a threshold function [16]. The width of the signal Gaussian is obtained from  $B \rightarrow J/\psi X_s$  data. The background shape is obtained from the background MC

sample. We verify the consistency of the background shape by comparing data and MC for  $B \rightarrow X_s e \mu$  combinations, for which we do not expect a signal. The fit results are given in Table I; we find  $60.1 \pm 13.9(\text{stat}) \pm 5.4(\text{syst})$  events for the combined  $B \rightarrow X_s \ell^+ \ell^-$  modes with a statistical significance of  $5.4\sigma$ . Here, the systematic error is obtained as a maximum deviation when the PDF parameters are varied by their standard deviations. The significance is defined as  $\sqrt{-2 \ln(\mathcal{L}_0 / \mathcal{L}_{\text{max}})}$ , where  $\mathcal{L}_{\text{max}}$  is the maximum likelihood and  $\mathcal{L}_0$  is the maximum likelihood when the signal yield is constrained to be zero. The fake background and the uncertainty in the background shape are included in the significance calculation. We calculate the branching fraction for  $M_{\ell^+ \ell^-} > 0.2 \text{ GeV}/c^2$  to be

$$\mathcal{B}(B \rightarrow X_s \ell^+ \ell^-) = (6.1 \pm 1.4(\text{stat}) \pm 1.4(\text{syst})) \times 10^{-6},$$

where the systematic errors in the yield, efficiency, the number of  $B$  meson pairs and the model errors are added in quadrature to give the total systematic error. Table I summarizes the branching fractions for  $B \rightarrow X_s e^+ e^-$  and  $B \rightarrow X_s \mu^+ \mu^-$  separately, together with the number of candidates, signal yields, fake background estimations, efficiencies and the statistical significances.

A cross-check is performed by replacing  $\Delta E$  with  $M_{\text{bc}}$  in the likelihood ratio criteria, and extracting the yield from the  $\Delta E$  distribution. We find a consistent signal yield using the same fitting functions for the signal and background as the ones used as the PDFs for  $\Delta E$ .

The dilepton mass spectrum is measured by dividing the data into  $M_{\ell^+ \ell^-}$  bins. For each bin, the signal yield is extracted from a fit to the  $M_{\text{bc}}$  distribution and the fake background contribution is subtracted. The result is shown in Fig. 1(c). Similarly, the recoil mass spectrum is obtained by dividing the data into  $M_{X_s}$  bins and extracting the signal yield for each bin. The result is shown in Fig. 1(d); the  $B \rightarrow K \ell^+ \ell^-$  signal is clearly seen,  $B \rightarrow K^* \ell^+ \ell^-$  is not significant, and we have additional contributions for  $M_{X_s} > M_{K^*}$ . With the current statistics, the  $M_{\ell^+ \ell^-}$  and  $M_{X_s}$  spectra are in agreement with the SM expectations. Branching fractions for each bin are given in Table II.

In summary, we present the first measurement of the inclusive branching fraction for the electroweak penguin decay  $B \rightarrow X_s \ell^+ \ell^-$ . The results on the branching fraction, dilepton and recoil mass spectra are in agreement with the SM expectations and can be used to constrain extensions of the SM.

We wish to thank the KEKB accelerator group for the excellent operation of the KEKB accelerator. We thank A. Ali, E. Lunghi and G. Hiller for providing us many helpful suggestions and calculations. We acknowledge support from the Ministry of Education, Culture, Sports, Science, and Technology of Japan and the Japan Society for the Promotion of Science; the Australian Research Council and the Australian Department of Industry, Science and Resources; the National Science Foundation of China under contract No. 10175071; the Department of Science and Technology of India; the BK21 program of the Ministry of Education of Korea and the CHEP SRC program of the Korea Science and Engineering Foundation; the Polish State Committee for Scientific Research under contract No. 2P03B 17017; the Ministry of Science and Technology of the Russian Federation; the Ministry of Education, Science and Sport of the Republic of Slovenia; the National Science Council and the Ministry of Education of Taiwan; and the U.S. Department of Energy.

---

\* on leave from Nova Gorica Polytechnic, Nova Gorica

<sup>†</sup> on leave from University of Toronto, Toronto ON

- [1] K. Abe *et al.* (Belle Collaboration), Phys. Rev. Lett. **88**, 021801 (2002).
- [2] For example, E. Lunghi, A. Masiero, I. Scimemi and L. Silverstrini, Nucl. Phys. **B568**, 120 (2000); J. L. Hewett and J. D. Wells, Phys. Rev. **D55**, 5549 (1997); T. Goto, Y. Okada, Y. Shimizu and M. Tanaka, Phys. Rev. **D55**, 4273 (1997); G. Burdman, Phys. Rev. **D52**, 6400 (1995); N. G. Deshpande, K. Panose and J. Trampetić, Phys. Lett. **B308**, 322 (1993); W. S. Hou, R. S. Willey and A. Soni, Phys. Rev. Lett. **58**, 1608 (1987).
- [3] C. Bobeth, M. Misiak and J. Urban, Nucl. Phys. **B574**, 291 (2000); H. H. Asatrian, H. M. Asatrian, C. Greub and M. Walker, Phys. Lett. **B507**, 162 (2001).
- [4] K. Abe *et al.* (Belle Collaboration), Phys. Lett. **B511**, 151 (2001).
- [5] S. Chen *et al.* (CLEO Collaboration), Phys. Rev. Lett. **87**, 251807 (2001).
- [6] R. Barate *et al.* (ALEPH Collaboration), Phys. Lett. **B429**, 169 (1998).
- [7] A. Ali, E. Lunghi, C. Greub and G. Hiller, hep-ph/0112300; A. Ali, P. Ball, L. T. Handoko and G. Hiller, Phys. Rev. **D61**, 074024 (2000).
- [8] E. Kikutani ed., KEK Preprint 2001-157 (2001), to appear in Nucl. Instr. and Meth. A.
- [9] A. Abashian *et al.* (Belle Collaboration), Nucl. Instr. and Meth. **A479**, 117 (2002).
- [10] R. A. Fisher, Annals Eugen. **7**, 179 (1936).
- [11] The Fox-Wolfram moments were introduced in G. C. Fox and S. Wolfram, Phys. Rev. Lett. **41**, 1581 (1978). The modified moments used by Belle are described in [4].
- [12] A. Ali, G. Hiller, L. T. Handoko and T. Morozumi, Phys. Rev. **D55**, 4105 (1997).
- [13] T. Sjöstrand, “PYTHIA 5.6 and JETSET 7.3: Physics and manual”, CERN-TH-6488-92.
- [14] D. Cronin-Hennessy *et al.* (CLEO Collaboration), Phys. Rev. Lett. **87**, 251807 (2001).
- [15] Calculated by the original authors based on Ref. [7].
- [16] H. Albrecht *et al.* (ARGUS Collaboration), Phys. Lett. **B229**, 304 (1989).

TABLE I: Fit results for the number of candidates, signal yields, fake backgrounds, reconstruction efficiencies, statistical significances and branching fractions ( $\mathcal{B}$ ). Candidates are counted in a  $\pm 3\sigma_{bc}$  window in  $M_{bc}$ .

mode	candidates	signal yield	fake background	efficiency (%)	significance	$\mathcal{B}(\times 10^{-6})$
$B \rightarrow X_s e^+ e^-$	96	$25.5 \pm 11.2^{+4.8}_{-3.8}$	$0.1 \pm 0.05$	$3.9 \pm 0.4 \pm 0.5$	3.4	$5.0 \pm 2.3^{+1.3}_{-1.1}$
$B \rightarrow X_s \mu^+ \mu^-$	92	$37.3 \pm 9.7^{+7.2}_{-3.8}$	$2.6 \pm 0.2$	$3.6 \pm 0.4 \pm 0.5$	4.7	$7.9 \pm 2.1^{+2.1}_{-1.5}$
$B \rightarrow X_s \ell^+ \ell^-$	188	$60.1 \pm 13.9^{+8.6}_{-5.4}$	$2.7 \pm 0.2$	$3.7 \pm 0.4 \pm 0.5$	5.4	$6.1 \pm 1.4^{+1.4}_{-1.1}$

TABLE II: Branching fractions ( $\mathcal{B}$ ) for each bin of  $M_{\ell^+ \ell^-}$  and  $M_{X_s}$ . Only the statistical error is given.

$M_{\ell^+ \ell^-}(\text{GeV}/c^2)$	$\mathcal{B}(\times 10^{-6})$	$M_{X_s}(\text{GeV}/c^2)$	$\mathcal{B}(\times 10^{-6})$
0.2 — 1.0	$0.93 \pm 0.74$	0.4 — 0.6	$0.49 \pm 0.14$
1.0 — 2.0	$1.12 \pm 0.66$	0.6 — 0.8	$-0.06 \pm 0.10$
$2.0 — M_{J/\psi}$	$1.87 \pm 0.76$	0.8 — 1.0	$0.52 \pm 0.34$
$M_{J/\psi} — M_{\psi'}$	$1.03 \pm 0.37$	1.0 — 1.6	$2.68 \pm 0.95$
$M_{\psi'} — 5.0$	$1.11 \pm 0.54$	1.6 — 2.1	$2.68 \pm 1.38$

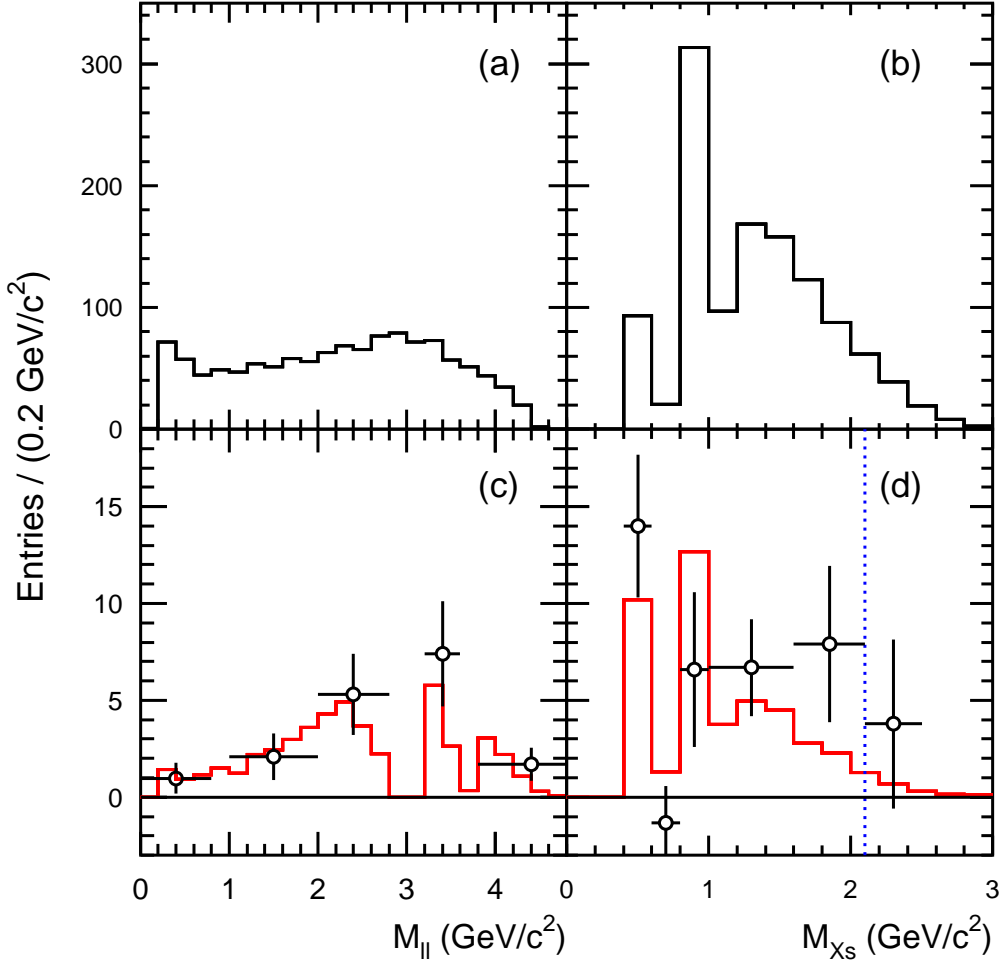


FIG. 1: SM expectations for the (a) dilepton and (b) recoil mass spectra; the observed (c) dilepton and (d) recoil mass spectra (circles). The histograms in (c), (d) show the SM expectations after all the selections are applied; histograms are normalized to the expected branching fractions. The dotted line in (d) indicates the  $M_{X_s} < 2.1$  GeV/c<sup>2</sup> requirement.

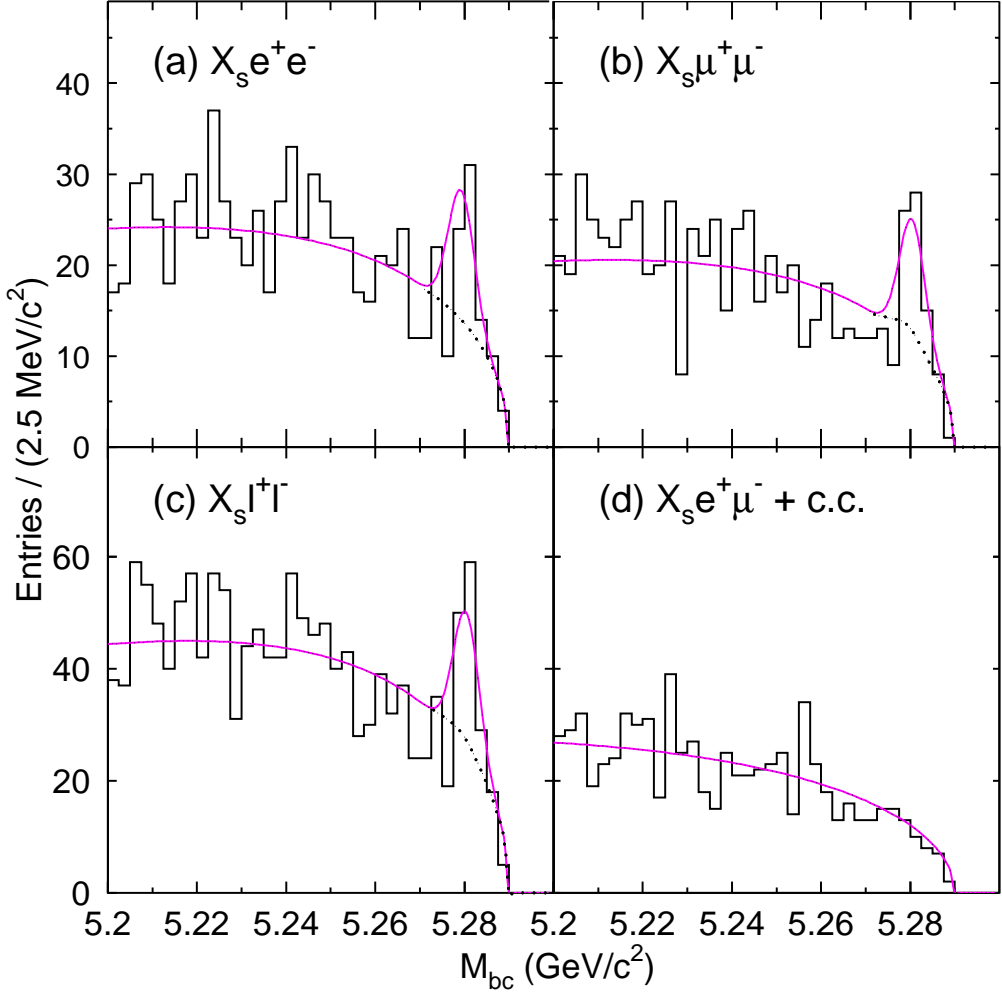


FIG. 2: Beam-energy constrained mass distributions for (a)  $B \rightarrow X_s e^+ e^-$ , (b)  $B \rightarrow X_s \mu^+ \mu^-$ , (c)  $B \rightarrow X_s \ell^+ \ell^-$  and (d)  $B \rightarrow X_s e^\pm \mu^\mp$ . The solid lines indicate the fit results and the dotted lines show the sum of the background components.